Efficient Red-Emitting Electrophosphorescent Polymers

Xiao-Hui Yang,[†] Fang-Iy Wu,[†,‡,§] Dieter Neher,[*,†] Chen-Han Chien,[‡] and Ching-Fong Shu[*,‡]

Institute of Physics, University of Potsdam, Am Neuen Palais 10, 14469 Potsdam, Germany, and Department of Applied Chemistry, National Chiao Tung University, Hsinchu 300, Taiwan

We report the synthesis and characterization of a series of electrophosphorescent polymers with a polyfluorene backbone, containing a red-emitting iridium complex and carrier-transporting units as the substitutes of the C-9 position of fluorene. Different specimens and contents of the hole-transporting moieties were found to influence the electroluminescent properties of the polymers. Incorporation of a hole-transporting/electron-blocking interfacial layer and utilization of an efficient electron injection cathode led to the saturated red-emitting electrophosphorescent polymer devices with the peak luminance efficiency and power conversion efficiency of 9.3 cd A^{-1} and 10.5 lm W^{-1}, respectively. The efficiencies were 8 cd A^{-1}/8 lm W^{-1} and 5.9 cd A^{-1}/4.6 lm W^{-1}, respectively, at 100 and 1000 cd m^{-2}.

Introduction

Electrophosphorescence with organometallic emitters has attracted substantial attention for both the singlet and the triplet excited states can contribute to light emission, allowing the internal quantum efficiency of light emitting devices to approach unity.[1] Further, the emission colors of these emitters can be tuned by changing the chemical structures of the ligands. Three primary color small molecule multilayer electrophosphorescent devices have shown impressive external quantum efficiencies (EQEs) and power conversion efficiencies (PCEs).[2]

Polymeric electrophosphorescent devices are attractive, in particular, for they offer the advantage of integrating the solution processability of polymer light emitting diodes (PLEDs) and the high efficiency of electrophosphorescence. Generally, there are two approaches to realize the polymer-based electrophosphorescent devices: physically or chemically blending phosphors with polymeric hosts. Efficiencies of the polymeric electrophosphorescent devices based on the former approach are pursuing those of small molecule multilayer electrophosphorescent devices.[3] We recently demonstrated solution-processable green-emitting polymeric

electrophosphorescent devices with a peak EQE of 18.8%, only slightly lower than the best reported values of the electrophosphorescent devices based on small molecules.[3m] Utilization of electrophosphorescent polymers makes for ease of device fabrication and is expected to effectively avoid the risk of phase separation of physically blending.

Electrophosphorescent polymers with both nonconjugated[4] and conjugated backbones[5] have been reported previously. Tokito et al.[4] reported polymers with an Ir complex and

* Corresponding authors. E-mail: neher@rz.unipotsdam.de (D.N.); shu@cc.nctu.edu.tw (C.-F.S.).
† University of Potsdam.
‡ National Chiao Tung University.
§ Current address: Department of Chemistry, National Tsing Hua University, Hsinchu 300, Taiwan.

(1) Baldo, M. A.; O'Brien, D. F.; You, Y.; Shoustikov, A.; Sibley, S.; Thompson, M. E.; Forrest, S. R. *Nature* **1998**, *395*, 151.
(2) (a) Lamansky, S.; Djurovich, P.; Murphy, D.; Razzaq, F. A.; Lee, H.-E.; Adachi, C.; Burrows, P. E.; Forrest, S. R.; Thompson, M. E. *J. Am. Chem. Soc.* **2001**, *123*, 4304. (b) Su, Y. J.; Huang, H. L.; Li, C. L.; Chien, C. H.; Tao, Y. T.; Chou, P. T.; Datta, S.; Liu, R. S. *Adv. Mater.* **2003**, *15*, 884. (c) Adachi, C.; Kwong, R. C.; Djurovich, P.; Adamovich, V.; Baldo, M. A.; Thompson, M. E.; Forrest, S. R. *Appl. Phys. Lett.* **2001**, *79*, 2082. (d) Tsuboyama, A.; Iwawaki, H.; Furugori, M.; Mukaide, T.; Kamatani, J.; Igawa, S.; Moriyama, T.; Miura, S.; Takiguchi, T.; Okada, S.; Hoshino, M.; Ueno, K. *J. Am. Chem. Soc.* **2003**, *125*, 12971. (e) Holmes, R. J.; D'Andrade, B. W.; Forrest, S. R.; Ren, X. R.; Li, J.; Thompson, M. E. *Appl. Phys. Lett.* **2003**, *83*, 3818.

(3) (a) Yang, M. J.; Tsutsui, T. *Jpn. J. Appl. Phys.* **2000**, *39*, L828. (b) Kawamura, Y.; Yanagida, S.; Forrest, S. R. *J. Appl. Phys.* **2002**, *92*, 87. (c) Yang, X. H.; Neher, D.; Hertel, D.; Däubler, T. K. *Adv. Mater.* **2004**, *16*, 161 and references therein. (d) Jiang, C. Y.; Yang, W.; Peng, J. B.; Xiao, S.; Cao, Y. *Adv. Mater.* **2004**, *16*, 537. (e) Yang, X. H.; Neher, D. *Appl. Phys. Lett.* **2004**, *84*, 2476. (f) Wu, F.-I.; Shih, P.-I.; Shu, C.-F.; Tung, Y.-L.; Chi, Y. *Macromolecules* **2005**, *38*, 9028. (g) Choulis, S. A.; Choong, V. E.; Mathai, M. K.; So, F. *Appl. Phys. Lett.* **2005**, *87*, 113503. (h) Wu, F.-I.; Su, H.-J.; Shu, C.-F.; Lo, L.-Y.; Diau, W.-G.; Cheng, C.-H.; Duan, J.-P.; Lee, G.-H. *J. Mater. Chem.* **2005**, *15*, 1035. (i) Liu, H. M.; He, J.; Wang, P. F.; Xie, H. Z.; Zhang, X. H.; Lee, C. S.; Sun, B. Q.; Xia, Y. J. *Appl. Phys. Lett.* **2005**, *87*, 221103. (j) Wu, F.-I.; Shih, P.-I.; Tseng, Y.-H.; Chen, G.-Y.; Chien, C.-H.; Shu, C.-F.; Tung, Y.-L.; Chi, Y.; Jen, A. L.-Y. *J. Phys. Chem. B* **2005**, *109*, 14000. (k) Suzuki, M.; Tokito, S.; Sato, F.; Igarashi, T.; Kondo, K.; Koyama, T.; Yamaguchi, T. *Appl. Phys. Lett.* **2005**, *86*, 103507. (l) Yang, X. H.; Jaiser, F.; Klinger, S.; Neher, D. *Appl. Phys. Lett.* **2006**, *88*, 021107. (m) Yang, X. H.; Muller, C. D.; Neher, D.; Meerholz, K. *Adv. Mater.* **2006**, *18*, 948. (n) Jou, J.-H.; Sun, M.-C.; Chou, H.-H.; Li, C.-H. *Appl. Phys. Lett.* **2006**, *88*, 141101. (o) Kim, S. W.; Park, J. H.; Oh, S. S.; Kim, D. Y.; Choi, E. H.; Cho, G. S.; Seo, Y. H.; Kang, S. O.; Park, B.; Saito, Y.; Watanabe, N.; Takezoe, H.; Watanabe, J. *Appl. Phys. Lett.* **2006**, *89*, 213511. (p) Liu, M.-S.; Niu, Y. H.; Luo, J. D.; Chen, B. Q.; Kim, T. D.; Bardecker, J.; Jen, A. K.-Y. *Polym. Rev.* **2006**, *46*, 7. (q) Wu, F.-I.; Shih, P.-I.; Tseng, Y.-H.; Shu, C.-F.; Tung, Y.-L.; Chi, Y. *J. Mater. Chem.* **2007**, *17*, 167.
(4) Tokito, S.; Suzuki, M.; Sato, F.; Kamachi, M.; Shirane, K. *Org. Electron.* **2003**, *4*, 105.
(5) (a) Chen, X. W.; Liao, J. L.; Liang, Y. M.; Ahmed, M. O.; Tseng, H. E.; Chen, S. A. *J. Am. Chem. Soc.* **2003**, *125*, 636. (b) Jiang, J. X.; Jiang, C. Y.; Yang, W.; Zhen, H. Y.; Huang, F.; Cao, Y. *Macromolecules* **2005**, *38*, 4072. (c) Sandee, A. J.; Williams, C. K.; Evans, N. R.; Devies, J. E.; Boothby, C. E.; Kohler, A.; Friend, R. H.; Holmes, A. B. *J. Am. Chem. Soc.* **2004**, *126*, 7041. (d) Zhen, H. Y.; Jiang, C. Y.; Yang, W.; Jiang, J. X.; Huang, F.; Cao, Y. *Chem. Eur. J.* **2005**, *11*, 5007. (e) Zhen, H. Y.; Luo, C.; Yang, W.; Song, W. Y.; Du, B.; Jiang, J. X.; Jiang, C. Y.; Zhong, Y.; Cao, Y. *Macromolecules* **2006**, *39*, 1693.

N-vinylcarbazole attached on a nonconjugated backbone. The EQEs of the resulting devices were 5.5, 9, and 3.5% for red, green, and blue, respectively. Electrophosphorescent polymers based on a polyfluorene (PF) backbone with a diketone pendant attached to the C-9 position of fluorene were reported by Chen et al.[5a] The devices based on the PF containing 1.3 mol % bis[2-(2′-benzothienyl)pyridinato-*N*,*C*[3′])(acetylacetonato)iridium complex unit exhibited the peak luminance efficiency (LE) of 2.8 cd A^{-1} at a voltage of 7.0 V and a luminance of 65 cd m^{-2} with the peak emission at 610 nm. Electrophosphorescent fluorene-*alt*-carbazole copolymers were synthesized by Jiang et al.[5b] in which cyclometalated Ir complexes with 1-phenylisoquinoline, 2-naphthylpyridine, and 2-phenylquinoline were grafted on the N-position of carbazole through a diketone-ended alkyl chain. Incorporation of the diketone-alkyl group onto the N-position of a carbazole unit was suggested to raise the flexibility and reactivity of the diketone group to the iridium core. Further, addition of carbazole in the backbone was shown to raise the highest occupied molecular orbital (HOMO) energy levels of the resulting polymers, making the hole injection easier. Devices of the copolymer bearing 0.5 mol % 1-phenylisoquinoline−Ir complex blended with 30 wt % electron-transporting 2-(4-biphenylyl)-5-(4-*tert*-butylphenyl)-1,3,4-oxadiazole (PBD) showed the maximum EQE of 4.9% (4.0 cd A^{-1}) at a current density of 5.9 mA cm^{-2} (7.7 V) and a luminance of 240 cd m^{-2} with the peak emission at 610 nm. A series of oligo- and polyfluorenyl bis-cyclometalated iridium complexes with the chemical formulas of [Ir(ppy-(FO)$_n$)$_2$(acac)] and [Ir(btp-(FO)$_n$)$_2$(acac)], where ppy is 2-phenylpyridinato, btp is 2-(2′-benzo[*b*]thienyl)pyridinato, acac is acetylacetonate, and FO is oligo(9,9-dioctylfluorenyl-2,7-diyl), were prepared by Sandee et al.[5c] The maximum EQEs of the devices based on [Ir(ppy-(FO)$_n$)$_2$(acac)] and [Ir(btp-(FO)$_n$)$_2$(acac)] were 0.12% and 1.5%, respectively. Bis(2-*p*-tolylpyridine-*C*[2′],*N*)-2,2,6,6-tetramethyl-3,5-heptanedioneiridium was introduced into the backbone of the fluorene-*alt*-carbazole copolymer, and an EQE of 4.1% (6.1 cd A^{-1}) was achieved at a current density of 32.2 mA cm^{-2} (13 V) and a luminance of 1730 cd m^{-2} with the peak emission at 575 nm.[5d] More recently, Zhen et al.[5e] reported electrophosphorescent chelating polymers based on the linkage isomers of 2-(1-naphthalene)pyridine and 2-(2-naphthalene)pyridine−bicycloiridium complexes: the resultant devices showed a saturated red emission with an EQE of 6.5% (2.5 cd A^{-1}) at 15 V and a luminance of 926 cd m^{-2} with the peak emission at 630 nm. The overall performances of the electrophosphorescent polymer devices are still inferior to those of the devices based on blending the phosphors with the polymeric hosts.[3]

We reported a PF copolymer with electron-transporting oxidiazole (OXD) and hole-transporting triphenylamine (TPA) moieties functioned at the C-9 position of fluorene, which exhibited stable blue emission and improved electroluminescent (EL) efficiency. It was further shown that the sp^3 carbon (C-9) of fluorene, serving as a spacer, effectively blocked the conjugation between the carrier-transporting

pendants and the fluorene unit.[6] Therefore, the functionalization at the C-9 position of fluorene can be well-adapted to synthesize electrophosphorescent PFs with the expectation of improved EL properties as a result of the facilitation of the carrier injection and transporting by the coexistence of the pendant carrier-transporting moieties.

In this paper we wish to report the synthesis and characterization of several electrophosphorescent PF derivatives with a red-emitting Ir complex and carrier-transporting moieties as the substitutes of the C-9 position of fluorene. A clear correlation between the performances of the devices and the properties of the pendant hole-transporting moieties was established. Further, the incorporation of a hole-transporting/electron-blocking interfacial layer and the utilization of an efficient electron injection cathode led to the saturated red-emitting electrophosphorescent polymer devices with the maximum LE of 9.3 cd A^{-1} and PCE of 10.5 lm W^{-1}.
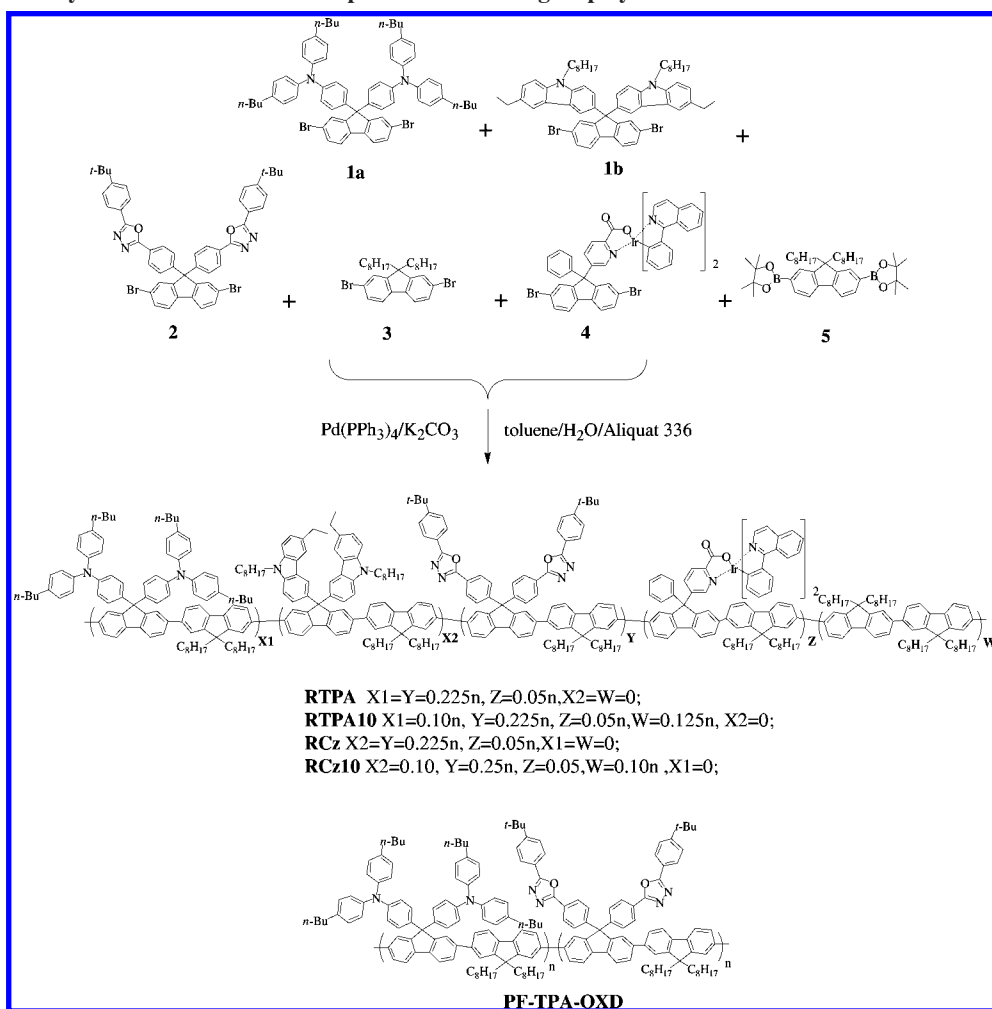
Experimental Section

Characterization. ^{1}H NMR spectra were recorded on a Varian UNITY INOVA AS500 (500 MHz for ^{1}H) spectrometers. Size exclusion chromatography was performed using a Waters chromatography unit interfaced with a Waters 410 differential refractometer; three 5 *μ*m Waters styragel columns (300 × 7.8 mm) were connected in series in order of decreasing pore size (10^4, 10^3, and 10^2 Å); tetrahydrofuran was the eluent. Standard polystyrene samples were used for calibration. Differential scanning calorimetry (DSC) was performed using a SEIKO EXSTAR 6000DSC unit at a heating rate of 20 °C min^{-1} and a cooling rate of 40 °C min^{-1}. Samples were scanned from 30 to 330 °C, cooled to 0 °C, and then scanned again from 30 to 330 °C. The glass transition temperatures were determined from the second heating scan. UV–vis spectra were measured using an HP 8453 diode-array spectrophotometer.

General Procedures of Polymerization. Red-emitting electrophosphorescent PF copolymer with 45 mol % TPA **(RTPA)** is taken as an example. To a solution of **1a** (59.1 mg, 57.0 *μ*mol), **2** (50.0 mg, 57.0 *μ*mol), **4** (14.2 mg, 12.7 *μ*mol), and **5** (81.4 mg, 126.7 *μ*mol) in toluene (2.0 mL) were added aqueous potassium carbonate (2.0 M, 1.0 mL) and Aliquat 336 (30 mg). The above solution was degassed, and tetrakis(triphenylphosphine)palladium (ca. 3 mg) was added in one portion under a nitrogen atmosphere. The solution was stirred at 90−95 °C for 36 h. The end groups were capped by refluxing for 12 h each with phenylboronic acid (17 mg, 140 *μ*mol) and bromobenzene (22 mg, 140 *μ*mol). After this period, the mixture was cooled and poured into a mixture of methanol and water (50 mL, 2:1 v/v). The crude polymer was filtered, washed with excess methanol, and dried. The polymer was dissolved in CHCl$_3$ and then precipitated twice into methanol. The precipitate was collected, washed with acetone for 24 h using a Soxhlet apparatus, and dried under vacuum. ^{1}H NMR (500 MHz, CDCl$_3$): δ 0.72–0.96 (m), 1.07 (br), 1.34 (br), 1.55 (br), 2.04 (br), 2.52 (br), 6.22–6.69 (m, ArH of Ir(piq)), 6.80–8.20 (m), 8.77–8.92 (m, ArH of Ir(piq)). Anal. Calcd: C, 85.78; H, 7.66; N, 3.50. Found: C, 84.04; H, 7.99; N, 4.13. The yields of **RTPA** and the following PF copolymers were 66−90%.

(6) (a) Wu, F.-I.; Reddy, D. S.; Shu, C.-F.; Liu, M.-S.; Jen, A. K.-Y. *Chem. Mater.* **2003**, *15*, 269. (b) Shu, C.-F.; Dodda, R.; Wu, F.-I.; Liu, M.-S.; Jen, A. K.-Y. *Macromolecules* **2003**, *36*, 6698. (c) Yuan, M.-C.; Shih, P.-I.; Chien, C.-H.; Shu, C.-F. *J. Polym. Sci., Part A: Polym. Chem.* **2007**, *45*, 2925. (d) Wu, F.-I.; Yang, X. H.; Neher, D.; Dodda, R.; Tseng, Y.-H.; Shu, C.-F. *Adv. Funct. Mater.* **2007**, *17*, 1085.

Red-Emitting Electrophosphorescent Polymers

Chem. Mater., Vol. 20, No. 4, 2008 1631

Scheme 1. Synthetic Scheme for the Bipolar Red-Emitting Copolymers and the Structures of PF-TPA-OXD

RTPA X1=Y=0.225n, Z=0.05n,X2=W=0;
RTPA10 X1=0.10n, Y=0.225n, Z=0.05n,W=0.125n, X2=0;
RCz X2=Y=0.225n, Z=0.05n,X1=W=0;
RCz10 X2=0.10, Y=0.25n, Z=0.05,W=0.10n ,X1=0;

PF-TPA-OXD

RTPA10. ^{1}H NMR (500 MHz, CDCl$_3$): δ 0.70–0.94 (m), 0.96–1.24 (m), 1.35 (br), 1.55 (br), 2.06 (br), 2.52 (br), 6.21–6.70 (m, ArH of Ir(piq)), 6.80–8.20 (m), 8.77–8.93 (m, ArH of Ir(piq)). Anal. Calcd: C, 85.43; H, 7.91; N, 3.24. Found: C, 84.51; H, 7.86; N, 3.92.

RCz. ^{1}H NMR (500 MHz, CDCl$_3$): δ 0.56–1.30 (m), 1.34 (br), 1.82 (br), 1.98 (br), 2.73 (br), 4.21 (br), 6.21–7.04 (m, ArH of Ir(piq)), 7.15–8.23 (m), 8.77–8.92 (m, ArH of Ir(piq)). Anal. Calcd: C, 85.38; H, 7.80; N, 3.64. Found: C, 84.53; H, 8.17; N, 4.03.

RCz10. ^{1}H NMR (500 MHz, CDCl$_3$): δ 0.60–1.29 (m), 1.35 (br), 1.84 (br), 2.03 (br), 2.74 (br), 4.22 (br), 6.22–7.04 (m, ArH of Ir(piq)), 7.15–8.25 (m), 8.78–8.93 (m, ArH of Ir(piq)). Anal. Calcd: C, 85.05; H, 7.87; N, 3.52. Found: C, 84.33; H, 8.09; N, 3.94.

Fabrication of Light-Emitting Devices. Poly(styrenesulfonate)-doped poly(3,4-ethylenedioxythiophene) (PEDOT:PSS) was spin-coated from aqueous solution onto precleaned and O$_2$-plasma treated indium−tin−oxide (ITO) substrates, yielding layers with a thickness of approximately 50 nm as determined by a Dektak profilometer. The PEDOT:PSS layers were baked at 80 °C for 0.5 h to remove residual water. The emissive polymer layer was spin-coated from a chlorobenzene solution on top of the PEDOT:PSS or the PFB interlayer films. The thickness of the polymer layers was around 70 nm. The samples were then annealed at 80 °C for 30 min. The devices were completed by thermal deposition of a CsF (1 nm)/ metal cathodes. Current–voltage characteristics were measured with a Keithley 2400 SourceMeter. The brightness of the devices was recorded with a Minolta CS-100A ChromaMeter. EL spectra were measured using a charge coupled device fiber spectrometer (Ocean

Optics HR2000). With exception of the deposition of the PEDOT: PSS layer, all processes were carried out in a dry nitrogen atmosphere. For interlayer formation, poly(9,9-dioctylfluorene-*co*-bis-*N*,*N'*-(4-butylphenyl)-bis-*N*,*N'*-phenyl-1,4-phenylenediamine) (PFB, M_w = 100 000 g/mol, purchased from American Dye Sources), was spin-coated from a toluene solution (12 mg/mL) onto the prebaked PEDOT:PSS layer inside the glovebox. Then, the films were annealed at 200 °C for 1 h. The soluble part of the polymer layer was removed by spin-rinsing with chlorobenzene, the solvent used for the deposition of the emissive layer.

Results and Discussion

The synthesis of the electrophosphorescent PF copolymers is shown in Scheme 1. **RTPA** copolymer was prepared through a Suzuki coupling reaction between the diboronate **5** and the dibromides **1a**, **2**, and **4** in a mole ratio of 50:22.5:22.5:5.0 by using Pd(PPh$_3$)$_4$ as the catalyst and Aliquat 336 (methyltrioctylammonium) as the phase-transfer reagent in a mixture of toluene and aqueous K$_2$CO$_3$ solution (2.0 M). The TPA-based dibromide **1a** and OXD-based dibromide **2** were functioned as the hole- and electron-transporting monomers, respectively. The dibromide **4**, directly bearing a bis[1-phenylisoquinolinato-*C*^{2},*N*]iridium-(III) picolinate [Ir(piq)] unit at the C-9 position of fluorene, was served as a red-emitting monomer. When the polymerization was completed, the end groups of the polymer chains were capped by heating the mixture under reflux
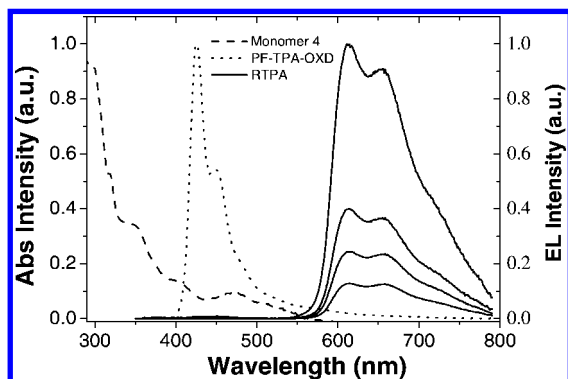
1632   *Chem. Mater., Vol. 20, No. 4, 2008*

Yang et al.

Figure 1. Absorption spectrum of monomer **4** in CHCl₃ solution, EL spectrum of **PF-TPA-OXD**, and EL spectra of the **RTPA**-based device at different current densities of 10, 20, 40, and 100 mA cm⁻² (from bottom to top).

Figure 2. Proposed energy level scheme for the devices having the configuration ITO/PEDOT:PSS/PFB interlayer/polymer/CsF/Al.

sequentially with phenylboronic acid and bromobenzene. Other PFs with various contents and specimens of the hole-transporting moieties were prepared following the same procedure as described for the synthesis of **RTPA**. The number-average molecular weights (M_n), obtained by gel permeation chromatography (GPC), were 4.6×10^4, 1.7×10^4, 3.1×10^4, and 3.9×10^4 g mol⁻¹ for **RTPA**, **RTPA10**, **RCz**, and **RCz10**, respectively, with polydispersities of 1.52–1.89. The iridium complex content in these copolymers was determined according to ¹H NMR spectra. In their ¹H NMR spectra, some weak resonances coming from the Ir(piq) units were found at δ 6.21–7.04 and 8.77–8.93, indicating the successful incorporation of the red phosphor into the resultant copolymers. The more downfield signals (δ 8.77–8.93) were assigned to the three aromatic protons ortho to the nitrogen atom in the three ligands of Ir(piq); therefore, the iridium complex content could be determined through comparing the integrations of the peaks from these aromatic protons with those from the aliphatic protons. The Ir complex content estimated from the NMR data was 4.0–4.7 mol %, which matched the monomer feed ratio agreeably. Here, the direct attachment of the phosphor unit to the polymer chain without utilizing the flexible alkyl chain linkage increases the rigidity of the polymers. For instance, the glass transition temperatures of **RTPA** and **RCz**, determined by using DSC, were 191 and 214 °C, respectively, significantly higher than those of the parent PF copolymers.[6b,c] Similar to **PF-TPA-OXD**, **RTPA** exhibits an absorption with a λ_{max} at 390 nm as a result of a $\pi-\pi^*$ absorption of the PF backbone; the additional absorption at around 300 nm can be attributed to the absorption of the pendant carrier-transporting moieties.[6] The absorption of the Ir(piq) units at longer wavelength (ca. 480 nm) is barely observable because of its low concentration in the copolymer and small extinction coefficient in this region.

As shown in Figure 1, the EL spectrum of **PF-TPA-OXD** overlaps well with the absorption spectrum of monomer **4**, which may imply that there is efficient energy transfer from the PF backbone to the Ir(piq) units in the **RTPA** films. Collaborating with this, a prevalent emission coming from the Ir(piq) units at 610 nm together with a minor contribution from the PF backbone at 425 nm was observed in the photoluminescence (PL) spectrum of **RTPA** films (not shown here).
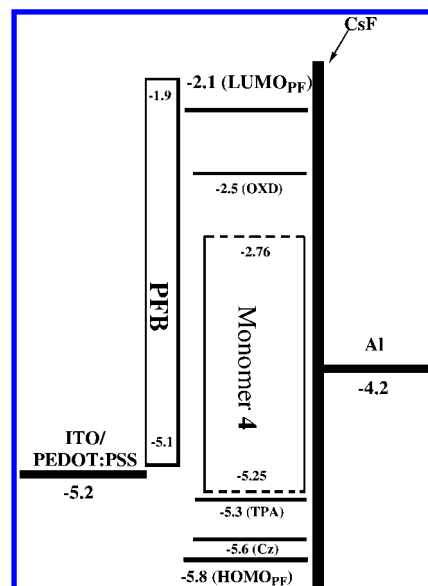
Cyclic voltammetry (CV) measurement of the monomer **4** was carried out to obtain information about the energy levels of the red-emitting parts of the PF copolymers, which then allows one to draw some general conclusions about the charge-transporting mechanisms in EL devices. For monomer **4**, an irreversible reduction, which occurred primarily on the electron-accepting heterocyclic portion of the cyclometalated piq ligands, was observed with the onset potential at −2.04 V, and a reversible oxidation, which mainly occurred at the Ir metal site, was found at 0.53 V with onset potential of 0.45 V. On the basis of the onset potentials of the oxidation and reduction, we estimated the HOMO and lowest unoccupied molecular orbital (LUMO) energy levels of monomer **4** with regard to the energy level of ferrocene (4.8 eV below vacuum).[7] The HOMO/LUMO levels of monomer **4** are calculated to be −5.25 and −2.76 eV, respectively. Figure 2 shows the energy level diagram for the complete devices based on the CV measurements of monomer **4**, **PF-TPA-OXD**, and **PF-Cz-OXD**.[6b,c]

The EL spectra of **RTPA** in the device configuration ITO/PEDOT:PSS/polymer/CsF/Al (device **A**) are also displayed in Figure 1. The EL spectra, which are independent of the driving current, are almost completely dominated by the emission from the Ir(piq) units, but a weak emission from the PF backbone can also be observed. Emission from the Ir(piq) units was more pronounced in the EL spectrum than in the PL spectrum indicating that the Ir complex containing moieties function as carrier traps in the EL process. It has been reported that carrier mobility of conjugated polymers can be significantly changed upon the incorporation of carrier-transporting moieties as side chains. Furthermore, the photoexcitation and field induction of the thermally stimulated current characteristics of the carbazole-grafted PF resemble those of the poly(N-vinylcarbazole) (PVK) other than the PF backbone, indicating that the carbazole moieties

(7) Pommerehne, J.; Vestweber, H.; Guss, W.; Mahrt, R. F.; Baessler, H.; Porsch, M.; Daub, J. *Adv. Mater.* **1995**, *7*, 551.
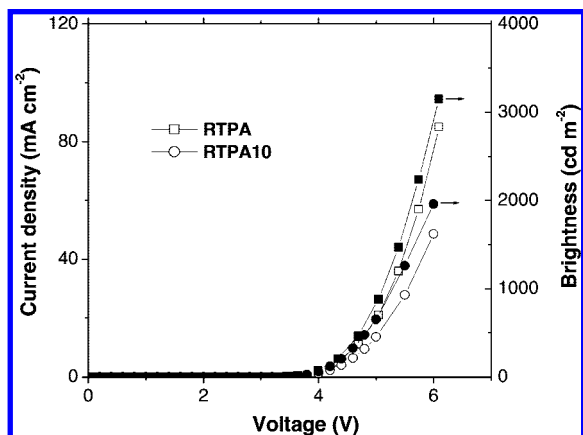
Red-Emitting Electrophosphorescent Polymers

Chem. Mater., Vol. 20, No. 4, 2008 1633

Figure 3. Plots of current density (open symbols) and luminance (solid symbols) as a function of the applied voltage for the **RTPA**- (squares) and **RTPA10**- (circles) based devices with the structure of PEDOT:PSS/polymer/CsF/Al.

play the dominating role in carrier transportation. Therefore, in the following discussion, the energy levels of Ir(piq) units were referenced to those of the carrier-transporting moieties, instead of those of the PF backbone.[8] According to the energy level diagram illustrated in Figure 2, the Ir(piq) units act as carrier trapping sites, especially for electrons in device **A**. The current density–voltage–luminance (I-V-L) characteristics of device **A** were plotted in Figure 3. The turn-on voltage (V_{on}) for device **A** was 2.8 V, and the peak LE and PCE were 4.2 cd A^{-1} and 3.1 lm W^{-1}, respectively. The Commission International de L'Eclairage (CIE) color coordinates were (0.67, 0.32). Table 1 summarizes the performances of the red-emitting electrophosphorescent polymer devices.

Through incorporating the carrier-transporting pendants, the **RTPA-**based device showed efficient and bright red electrophosphorescence at a lower operating voltage with respect to other efficient red electrophosphorescent polymer devices.[5a–c,e] However, we think there still remains some room for further improvement. Previously, we found that the EL efficiencies were improved by a factor of approximately 2 when doping a red iridium-based phosphor into **PF-OXD**, in which the TPA pendant groups of **PF-TPA-OXD** were replaced with the OXD groups, instead of doping it into **PF-TPA-OXD**.[3j] This result implied that the content of the TPA moieties in the copolymer was important for the performance of the devices. The hole mobility of TPA is at least 1 order of magnitude higher than the electron mobility of OXD.[9] The large difference of the hole and electron mobilities needs to be reconsidered in the present devices without the electron-transporting/hole-blocking layer. Recent studies also revealed that a less concentrated content

of the hole-transporting groups relative to that of the electron-transporting groups in the emissive layer can lead to the optimal EL efficiency of the phosphor-based PLEDs.[3k] Therefore, we prepared another copolymer **RTPA10** by diluting the TPA content in the **RTPA** copolymer to 10 mol % with dioctylfluorene units (see Scheme 1). The I-V-L properties of the **RTPA10**-based devices (device **B**) are displayed in Figure 3 for the sake of comparison. The V_{on} of device **B** was similar with that of device **A**. However, reducing the content of the TPA moieties led to improving the maximum LE of the devices to 5.2 cd A^{-1}, 20–30% higher than that of device **A**. The improvement of the EL efficiencies can be mainly attributed to more balanced hole and electron recombination on the Ir(piq) units resulted from the reduction of hole mobility.[3k]

Another approach to restrict direct discharging of holes at the cathode is to down shift the HOMO level of the hole-transporting moieties so that the Ir(piq) units would work as effective hole traps as well. Toward this, **RCz** was prepared by replacing the TPA groups of **RTPA** with the carbazole (Cz) groups, where the HOMO level of Cz was approximately 0.3 eV lower than that of the Ir(piq) unit (see Figure 2); therefore, holes may be potentially trapped by the Ir(piq) units. Figure 4 shows the I-V-L properties of the **RCz**-based devices (device **C**). The V_{on} of device **C** increased to 3.8 V as compared with device **A**, reflecting the increase of the energy barrier for hole injection. The EL spectrum of device **C** was similar to that of device **A** with the CIE color coordinates of (0.67, 0.32). The peak LE of device **C** was 5.7 cd A^{-1}. We note that the presence of a negative charge on the Ir(piq) unit will shift the HOMO level and vary the probability of hole–electron recombination. Reducing the content of Cz to 10 mol % (**RCz10**, see Scheme 1), for the variation of the hole injection and transporting, only slightly changed the device behaviors (device **D**), for example, marginal reduction of current densities at high driving voltages, indicating that hole trapping by the Ir(piq) units is dominant for hole transporting in the **RCz**- and **RCz10**-based devices (Figure 4).

Incorporation of an interfacial layer between the PEDOT:PSS and the emissive layer was shown to improve the performances of both polymeric electrofluorescent[10a] and electrophosphorescent light emitting devices.[3g,10b] In the **RCz**-based devices with a PFB interfacial layer (device **E**), the V_{on} was reduced to 3 V accompanied with the peak LE increased to 6.7 cd A^{-1} (Table 1). As depicted in Figure 4, device **E** showed a relatively lower current density with respect to device **C** at above 5 V, which may be attributed to the variation of hole injection in the devices or the electron-blocking ability of the PFB interfacial layer. Besides the emission from the Ir(piq) units, there was a trace of PFB emission in the EL spectra, the intensity of which slightly increased with increasing current density, clearly manifesting electron leakage to the PFB interfacial layer. Nevertheless, the CIE coordinates of device **E** at approximately 1000 cd m^{-2} were (0.66, 0.33), still located in the saturated red region. The appearance of PFB emission in the EL spectra suggests that the carrier recombination zone of the devices is situated close to the PFB/**RCz** interface. The energy

(8) Liu, C. Y.; Chen, S. A. *Macromol. Rapid Commun.* **2007**, *28*, 1743.
(9) (a) Pai, D. M.; Yanus, J. F.; Stolka, M. *J. Phys. Chem.* **1984**, *88*, 4714. (b) Tokuhisa, H.; Era, M.; Tsutsui, T.; Saito, S. *Appl. Phys. Lett.* **1995**, *66*, 3433.
(10) (a) Kim, J. S.; Friend, R. H.; Grizzi, I.; Burroughes, J. H. *Appl. Phys. Lett.* **2005**, *87*, 023506. (b) Yang, X. H.; Jaiser, F.; Stiller, B.; Neher, D.; Galbrecht, F.; Scherf, U. *Adv. Funct. Mater.* **2006**, *16*, 2156.
(11) (a) Brown, T. M.; Friend, R. H.; Millard, I. S.; Lacey, D. J.; Butler, T.; Burroughes, J. H.; Cacialli, F. *J. Appl. Phys.* **2003**, *93*, 6195. (b) Chan, M. Y.; Lai, S. L.; Fung, M. K.; Lee, C. S.; Lee, S. T. *J. Appl. Phys.* **2004**, *95*, 5397.

Table 1. Performances of the Red-Emitting Electrophosphorescent Polymer Devices[a]

ITO/PEDOT:PSS/polymer/cathode	V_{on}[b] [V]	LE [cd A^{-1}]	PCE [lm W^{-1}]	L_{20}[c] [cd m^{-2}]	CIE (x, y)[d]
RTPA/CsF/Al (device **A**)	2.8	4.2	3.1	880 @ 5 V	0.67, 0.32
RTPA10/CsF/Al (device **B**)	3.0	5.2	3.9	950 @ 5.4 V	0.67, 0.32
RCz/CsF/Al (device **C**)	3.8	5.7	3.7	1 100 @ 6.1 V	0.67, 0.32
RCz10/CsF/Al (device **D**)	3.6	5.5	3.7	1 040 @ 6.1 V	0.67, 0.32
PFB/**RCz**/CsF/Al (device **E**)	3.0	6.7	5.0	1 020 @ 6.8 V	0.66, 0.33
PFB/**RCz**/CsF/Ca/Al (device **F**)	2.2	9.3	10.5	1 150 @ 4.1 V	0.66, 0.33

[a] The data for LE and PCE are the maximum values of the devices. [b] The applied voltage required for 0.01 cd m^{-2}. [c] Luminance measured at 20 mA cm^{-2}. [d] CIEs at ca. 1000 cd m^{-2}.
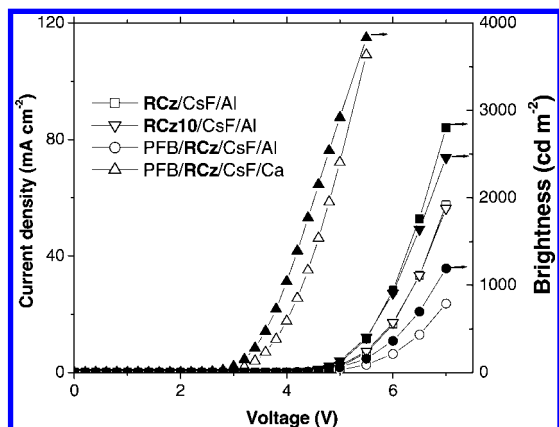

Figure 4. Plots of the current density (open symbols) and luminance (solid symbols) as a function of the applied voltage for PEDOT:PSS/**RCz**/CsF/Al (squares), PEDOT:PSS/**RCz10**/CsF/Al (down-triangles), PEDOT:PSS/PFB interlayer/**RCz**/CsF/Al (circles), and PEDOT:PSS/PFB interlayer/**RCz**/CsF/Ca/Al (up-triangles) devices.

barriers are 0.5 and 0.6 eV for holes and electrons, respectively, to traverse the PFB/**RCz** interface as shown in Figure 2, leading to good confinement of both holes and electrons at the interface. The improvement of the efficiencies of device **E** relative to device **C** was significant in the low current density regime. The efficiencies of device **E** were comparable with those of device **C** at high current densities where a high electric field nullified the energy barrier for carrier injection and the mobility of holes and electrons may become more matched. In addition, the probability of quenching emissive triplet excited states (triplet–triplet and polaron−triplet annihilation) may be increased in device **E** as a result of the accumulation of holes and electrons at the interface to the PFB layer and a resultant narrow carrier recombination zone. A similar variation of the device efficiencies was also observed in the PVK:PBD:(piq)$_2$Ir(acac)-based devices in conjunction with a PFB interfacial layer ((piq)$_2$Ir(acac), bis(1-phenylisoquinoline)(acetylacetonate)-iridium). Because of the same carrier-transporting moieties for the **RCz** and PVK:PBD:(piq)$_2$Ir(acac)-based devices and duplicated changes of the device behaviors upon incorporation of a PFB interfacial layer, we assume that the direct injection of holes from the HOMO level of PFB to that of the Ir(piq) units takes place in device **E**, as found in the PVK:PBD:(piq)$_2$Ir(acac)-based devices.[10b] Therefore, increasing the content of the Ir(piq) units would inhibit PFB emission, and the corresponding synthesis is ongoing.

The efficiencies of the **RCz**-based devices can be further improved by utilizing a CsF/Ca/Al cathode instead of a CsF/Al cathode. Previous study on the blue-emitting PF derivative devices showed that there was a considerable change in the polymer's electronic structure resulting from the reaction with the CsF/Ca cathode, leading to a low built-in potential of the devices and the appearance of the defect emission in the EL spectra.[11a] Indeed, the PEDOT:PSS/**RCz**/CsF/Ca/Al devices showed significantly larger current density under a certain operating voltage than those with a CsF/Al cathode but a rather low LE (2–3 cd A^{-1}). However, the EL efficiency of the devices was dramatically improved by addition of a PFB interfacial layer. The I-V-L characteristics of the **RCz**-based devices with a PFB interfacial layer and a CsF/Ca/Al cathode (device **F**) are presented in Figure 4. Compared with device **E**, the driving voltage for device **F** to achieve certain current density was significantly reduced, for example, by approximately 1.5 V for a current density of 50 mA cm^{-2}. Meanwhile, the luminance of device **F** increased sharply with the driving voltage increased: 3.1 V for 100 cd m^{-2} and 4 V for 1000 cd m^{-2}. The peak LE and PCE of device **F** were 9.3 cd A^{-1} (corresponding to an EQE of ca. 9%) and 10.5 lm W^{-1}, respectively, at a current density of 0.26 mA cm^{-2}, a driving voltage of 2.8 V, and a luminance of 24 cd m^{-2}. The LEs and PCEs at 100 and 1000 cd m^{-2} were 8 cd A^{-1}/8 lm W^{-1} and 5.9 cd A^{-1}/4.6 lm W^{-1}, respectively. This represents a significant improvement of the efficiencies of electrophosphorescent polymer devices. In fact, the overall performances of the devices are even comparable to those of the small molecule multilayer devices.[2b,d] The EL spectra of the device **F** were similar with those of the device **E**. We speculate that the opposite trends for the device performances of the PFB interfacial layer devices and of the PEDOT:PSS devices, when combined with a CsF/Ca/Al cathode, may be attributed to a well-defined carrier recombination zone in the former devices as discussed above, which may be far from the cathode metal doped region. Indeed, in the small molecule multilayer devices with a well-defined carrier recombination zone, utilization of CsF/low work-function metal cathodes was shown to improve both the PCE and the lifetime of the devices.[11b]

The primary device lifetime testing is encouraging: device **F** showed less than a 10% drop of luminance for 10 h constant current driving with an initial luminance of approximately 150 cd m^{-2}, much better than what was observed in the PVK:PBD:(piq)$_2$Ir(acac)-based devices. Detailed long-time stress tests are required to clarify if phase separation in the latter devices plays a crucial role in the device degradation.

In conclusion, a series of electrophosphorescent PF copolymers with a red-emitting Ir complex and carrier-transporting moieties as the substitutes of the C-9 position of fluorene were synthesized. The contents and the specimens of the hole-transporting moieties were shown to be correlated

with the performances of electrophosphorescent polymer devices. Further incorporation of a hole-transporting/electron-blocking interfacial layer and utilization of an efficient electron injection cathode led to saturated red-emitting electrophosphorescent polymer devices with a peak LE of 9.3 cd A^{-1} and a PCE of 10.5 lm W^{-1}.

CM702789C